journal

J. Am. Ceram. Soc., 1–6 (2013)
DOI: 10.1111/jace.12685

AC Impedance Spectroscopy of CaF_2-doped AlN Ceramics

Hyeon-Keun Lee,[‡] Hyun Min Lee,[§] and Do Kyung Kim[§,†,*]

[‡]Product Engineering Laboratory, Samsung Corning Precision Materials Co., Ltd, No. 544 Myungam-ri, Tangjeong-myeon, Asan-city 336-725, Korea

[§]Department of Materials Science and Engineering, Korea Advanced Institute of Science and Technology (KAIST), 291 Daehak-ro, Yuseong-gu, Daejeon 305-701, Korea

The electrical conductivity of CaF_2-doped aluminum nitride (AlN) ceramics was characterized at high temperatures, up to 500°C, by AC impedance spectroscopy. High thermal conductive CaF_2-doped AlN ceramics were sintered with a second additive, Al_2O_3, added to control the electrical conductivity. The effects of calcium fluoride (CaF_2) on microstructure and related electrical conductivity of AlN ceramics were examined. Investigation into the microstructure of specimens by TEM analysis showed that AlN ceramics sintered with only CaF_2 additive have no secondary phases at grain boundaries. Addition of Al_2O_3 caused the formation of amorphous phases at grain boundaries. Addition of Al_2O_3 to CaF_2-doped AlN ceramics at temperatures 200°C–500°C revealed a variation in electrical resistivity that was four orders of magnitude larger than for the specimen without Al_2O_3. The amorphous phase at the grain boundary greatly increases the electrical resistivity of AlN ceramics without causing a significant deterioration of thermal conductivity.

I. Introduction

Aluminum nitride (AlN) ceramics are highly thermal conductive nonmetallic materials. Their unique properties, including high thermal conductivity, low dielectric constant, high electrical resistance, wide band gap (E_g = 6.2 eV at room temperature, RT), strong mechanical properties, chemical inertness, and similar thermal expansion coefficient to silicon, make AlN a promising candidate for electronic substrates and electrostatic chucks.[1–6]In recent decades, many studies have examined the thermal conductivity of AlN and its effect on microstructure under certain conditions.[7–9] However, few studies have considered the electrical conductivity, and the electrical conduction mechanism of AlN ceramics is not fully understood.[10,11] Francis and Worrell[12] reported the AC and DC electrical conductivity of hot-pressed polycrystalline AlN ceramics, and Richards *et al.*[13] investigated the electrical conductivity of BeO-doped hot-pressed AlN ceramics within atmospheres with varying nitrogen partial pressure, at temperatures 800°C–1200°C. The activation energy for electrical conduction was found to be between 1.45 and 1.57 eV and it was concluded that the charge carriers are intrinsic electrons or aluminum vacancies.

Controlling the electrical resistivity of AlN ceramics becomes important when the ceramics are used for electronic applications. The electrical resistivity must be maintained within the desired range while the thermal conductivity is kept high. Yoshikawa *et al.*[14] investigated the electrical resistivity of Sm_2O_3-doped AlN ceramics at RT using the DC three-pole method. They showed that the three-dimensional network of the grain-boundary phase of Sm-β-alumina enables the electrical resistivity of AlN ceramics to be controlled in the range 10^{10}–10^{14} Ω cm. Kusunose *et al.*[15] reported that by precipitating a yttrium oxycarbide grain-boundary phase, AlN ceramics can be electrically conductive ceramics without losing their intrinsic high thermal conductivity. These studies indicate that the variation in the electrical conductivity of AlN ceramics is determined by both the electrical properties and the structure of the secondary phase at grain boundaries; however, they did not investigate the electrical conductivity of AlN ceramics in detail.

In this study, we report on high-temperature AC impedance spectroscopy and the electrical properties of AlN ceramics, considering the existence of a grain-boundary amorphous phase. Highly thermally conductive AlN ceramics with a controlled grain-boundary phase were sintered using CaF_2 and Al_2O_3 as sintering additives.[16,17] CaF_2 sintering additives promote densification in low-temperature sintering by forming a liquid phase at a relatively low temperature. CaF_2 also reacts with other sintering additives and leaves a minimal amorphous second phase at the grain boundary, because the liquid phase evaporates at high temperatures. We assessed the effect on electrical resistivity of adding small amounts of Al_2O_3 to CaF_2-doped AlN ceramics.

II. Experimental Procedure

A commercial AlN powder (F grade; Tokuyama Corp., Tokyo, Japan) with an average particle size of 1.0 μm and specific surface area of 3.27 m^2/g was used in this experiment. AlN powder was mixed with calcium fluoride (CaF_2, Aldrich, Milwaukee, WI) and aluminum oxide (Al_2O_3, Aldrich, Milwaukee, WI) separately, and placed in a ball-mill for 24 h in a 2-propanol liquid medium. After mixing the starting materials, the slurry was dried. The dried powder was uniaxially pressed into a 20-mm-diameter disk under a pressure of 30 kg/cm^2, and was cold isostatic pressed at 200 MPa. The compacts were placed between two boron nitride plates. The specimens were then sintered via pressureless sintering in a graphite furnace (ASTRO Thermal Technology, Santa Barbara, CA) at 1900°C for 3 h in an N_2 atmosphere. The heating rate during the sintering was 10°C/min, and the cooling rate was 25°C/min.

The fracture surface of the sintered pellets was characterized by analysis with a field-emission scanning electron microscope (FE-SEM; Philips XL30 FEG, Eindhoven, the Netherlands). The internal microstructure was investigated by transmission electron microscopy (TEM; Tecnai G^2 F30 S-twin, FEI, Eindhoven, the Netherland).The samples were prepared by standard methods, which involved mechanical grinding to a thickness of approximately 50 μm, dimpling to approximately 10 μm, then ion beam milling to electron transparency. The compositions were measured by energy

H. Chan—contributing editor

Manuscript No. 33216. Received May 16, 2013; approved September 30, 2013.
*Member, The American Ceramic Society.
†Author to whom correspondence should be addressed. e-mail: dkkim@kaist.ac.kr

dispersive X-ray spectroscopy (EDXS).The thermal diffusivity was measured by the laser flash method using a Xenon Flash instrument (LFA 447 Nanoflash, Netzsch Instruments Inc., Burlington, VT).

For the impedance spectroscopy analysis, thin silver films were deposited on both sides of the specimen, which served as electrodes. The films were deposited on a circular area (1.0 mm diameter) at the center of the pellet. The silver electrode-coated specimen was sandwiched between platinum foil, which was connected to platinum wires in a spring-loaded specimen holder. The electrical properties were measured by impedance spectroscopy at an amplitude of 1000 mV (Solartron 1260, Farnborough, UK) over a decreasing frequency range from 13 MHz to 5 Hz, and over the temperature range 200°C–500°C for CaF_2-doped AlN ceramics. Impedance spectra were collected at 25°C intervals. The temperature was maintained for a sufficient time (20 min) to achieve thermal equilibration of the whole specimen at each temperature before the data were collected. The total impedance was resolved into real (Z') and imaginary (Z'') parts, and Cole–Cole plots were constructed to analyze the data.

To analyze the electrical properties of the polycrystalline AlN ceramics, the simplified brick layer model, in which a polycrystalline solid is represented by cubic grains separated by flat grain boundaries, was used. The number of RC (resistor–capacitor) branches in the equivalent circuit equals the number of different microstructural components in the ceramic, such as grains, grain boundaries, electrodes, precipitates, or pores. In the absence of any precipitates or electrode polarization effects, only the RC branches representing grains and grain boundaries exist. The grain resistivity (ρ_{grain}) and the net grain-boundary resistivity (ρ_{gb}) were calculated based on the following equations:

$$\rho_{grain} = R_{grain} \cdot A/t \quad (1)$$

$$\rho_{gb} = R_{gb} \cdot A/t \quad (2)$$

where A is the effective electrode area and t is the specimen thickness.

The specific grain-boundary resistivity ($\rho_{gb}{}^{sp}$) is the average resistivity of a single grain, which is theoretically related to the net grain-boundary resistivity (ρ_{gb}), the grain size (d_g), and the grain-boundary thickness (δ_{gb}), as

$$\rho_{gb}^{sp} = \sigma_{gb} \cdot d_g/\delta_{gb} \quad (3)$$

The actual contribution of a single grain boundary to the entire boundary resistivity is thus closely related to the boundary characteristics.

III. Results and Discussion

(1)Sinterability and Thermal Conductivity

The bulk density and thermal conductivity of the sintered specimens which were prepared with a CaF_2 additive system are shown in Fig. 1. Highly dense (>95%) and high thermal conductivity (190.4 W/mK) AlN ceramics were obtained with 3 wt% CaF_2 additives. The densification was conducted by means of liquid phase sintering with the CaF_2 additives. The role of CaF_2 as an additive was to react with Al_2O_3 on the surface of the AlN powder, and promote densification through sintering by means of eutectic melt in the CaF_2–Al_2O_3 system. Control of the atmosphere by covering with the boron nitride plate also promotes the densification of CaF_2-doped AlN ceramics.[15]

To control the electrical conductivity of AlN ceramics, a second additive, Al_2O_3, was used. Al_2O_3 additives at 1 and 3 wt% were added to 3 wt% CaF_2-doped AlN ceramics (C3A1 and C3A3, respectively).All specimens exhibited high

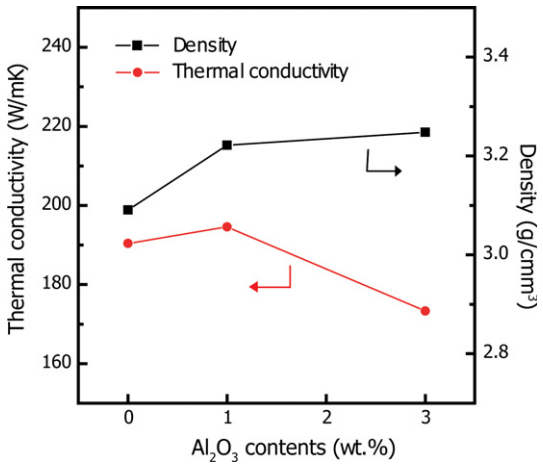

Fig. 1. Density and thermal conductivity of 3 wt% CaF_2-doped AlN ceramics with 0, 1, and 3 wt% added Al_2O_3.

density, over 3.10 g/cm^3. Addition of Al_2O_3 increases the density to 3.23 g/cm^3. It is known that the addition of a small amount of Al_2O_3 increases the thermal conductivity of the specimen by facilitating liquid phase sintering. However, a large amount of Al_2O_3 addition decreases the thermal conductivity because oxygen-related defects increase by the solid solution of Al_2O_3 into AlN grain, as confirmed here. The C3 specimen yielded the maximum thermal conductivity of 190.4 W/mK, and the C3A3 specimen yielded a value of 173.3 W/mK.

Figure 2 shows SEM micrographs of three sintered-AlN ceramics (specimens C3, C3A1, and C3A3). The second phases at the grain boundaries of AlN ceramics were not observed when CaF_2 and Al_2O_3 sintering additives were used. Because CaF_2 is volatile above 1600°C, the liquids phases composed of CaF_2 might be evaporated during high-temperature sintering. CaF_2 is supposed to react with AlN and form gas-phase Ca and AlF_3 as follows:

$$3CaF_2(s) + 2AlN(s) = 3Ca(g) + 2AlF_3(g) + N_2(g) \quad (4)$$

The vapor pressure of Ca(g) is sufficiently high (0.1 mbar) at 1600°C and AlF_3 begins to sublime at 1250°C.[18]. Therefore, there are no remaining phases at the grain boundaries after the sintering at 1900°C.

In AlN crystals, the most influential defects are oxygen-related defects, consisting of oxygen substitutions for nitrogen (O_N), aluminum vacancies (V_{Al}), and O_N–V_{Al} complexes. These defects become phonon scattering sources and can thus influence the electrical and thermal conductivity of the AlN grain. Figure 2 shows that the grain size of the specimen with Al_2O_3 additive is larger than that of the specimen without Al_2O_3. However, the grain size does not affect the thermal conductivity of the samples because the phonon mean free path of the high-thermal conductivity AlN ceramics is very small compared with the grain size.[19]

(2) Electrical Conductivity

Figure 3 shows the complex impedance spectra of the C3 and C3A3 specimens at 350°C. Three semicircles corresponding to the impedance response of the grain, the grain boundary, and the electrode are shown well within each graphs. From analysis of the impedance spectra, the grain-boundary resistivity of the C3 specimen observed is slightly higher than the grain resistivity. In contrast, the grain-boundary resistivity of C3A3 is much higher than the grain resistivity [Fig. 3(b)]. This indicates that the addition of

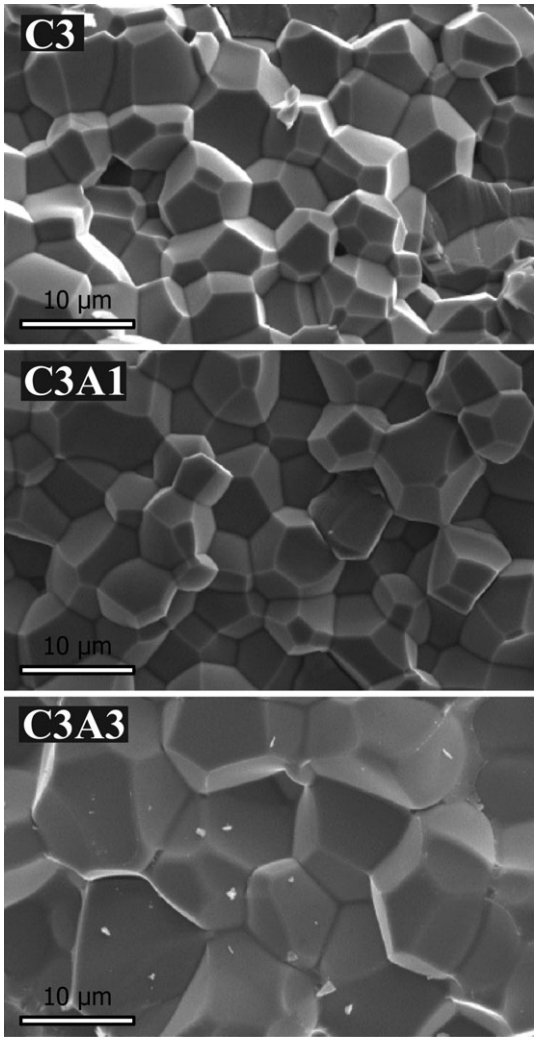

Fig. 2. SEM micrographs of a fracture surface in specimens C3, C3A1, and C3A3. The second phases at the grain boundaries were not observed in all specimens.

Al_2O_3 has an effect on grain-boundary resistivity. The C3A3 specimen has a higher grain-boundary resistivity than the C3 specimen. To analyze the relationship between the grain and grain-boundary resistivity, both are shown in Fig. 4(a). The resistivity of the grain boundary is up to four orders of magnitude higher than the grain resistivity. The resistivity of the grain boundary increases with increasing amounts of Al_2O_3; however, the variation in grain resistivity is much smaller than that in grain-boundary resistivity. The ratio of the grain-boundary resistivity to the grain resistivity is shown in Fig. 4(b) for the C3, C3A1, and C3A3 specimens, to investigate the grain-boundary blocking effect on electrical conduction. In Fig. 4(a), the grain-boundary resistivity of the C3A1 specimen is one order of magnitude higher than that of the C3 specimen, but the ratio of the grain-boundary resistivity to the grain resistivity is only a little higher than that of the C3 specimen. This means that the high electrical resistivity of the C3A1 specimen was caused by high grain resistivity, and the grain-boundary blocking effects were insignificant with a small amount of Al_2O_3 addition. However, the C3A3 specimen, which has a large amount of Al_2O_3, shows that the grain-boundary resistivity was 50–1000 times higher than the grain resistivity. The ratio of the grain-boundary resistivity to the grain resistivity for the C3A3 specimen (50–1000) is higher than that of the C3 specimen (5–10) in the measured temperature range. This reflects the high electrical resistivity of the C3A3 specimen, which was caused by the grain-boundary blocking effect on electrical conduction. In the CaF_2-doped AlN ceramics with 3 wt% Al_2O_3, the thermal conductivity decreases slightly due to the solid solution of Al_2O_3 into AlN grain (by <10%), but the electrical resistivity increases by up to three orders of magnitude.

(3) Internal Structure

Transmission electron microscopy analysis of the C3 and C3A3 specimens was conducted to investigate the cause of the grain-boundary blocking effect of the specimen with added Al_2O_3 (Fig. 5).In the TEM image of the C3 specimen, the grain boundaries are essentially clean [Fig. 5(a)].Analysis by high-resolution TEM (HRTEM) revealed that, the grain boundaries are well crystallized, and there are no segregation atoms or amorphous/glassy phases along grain boundaries [Fig. 5(b)]. The grain boundaries are free of any second phase, showing direct grain-to-grain contacts in the C3 specimen. Only aluminum and nitrogen elements were detected, and no calcium atoms were observed in the grain interior. In spite of clean grain boundaries, the value of the grain-boundary resistivity is still higher than that of the grain resistivity. The high grain-boundary resistivity can be explained to the

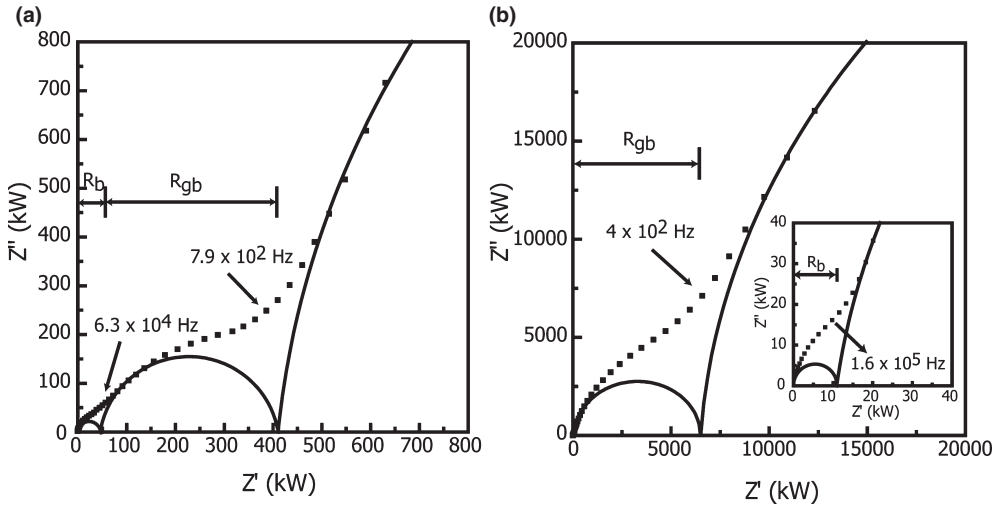

Fig. 3. Complex impedance spectra including three semicircles, which are corresponding to the impedance response of the grain, the grain boundary, and the electrode, of specimens C3 (a) and C3A3 (b) at 350°C.

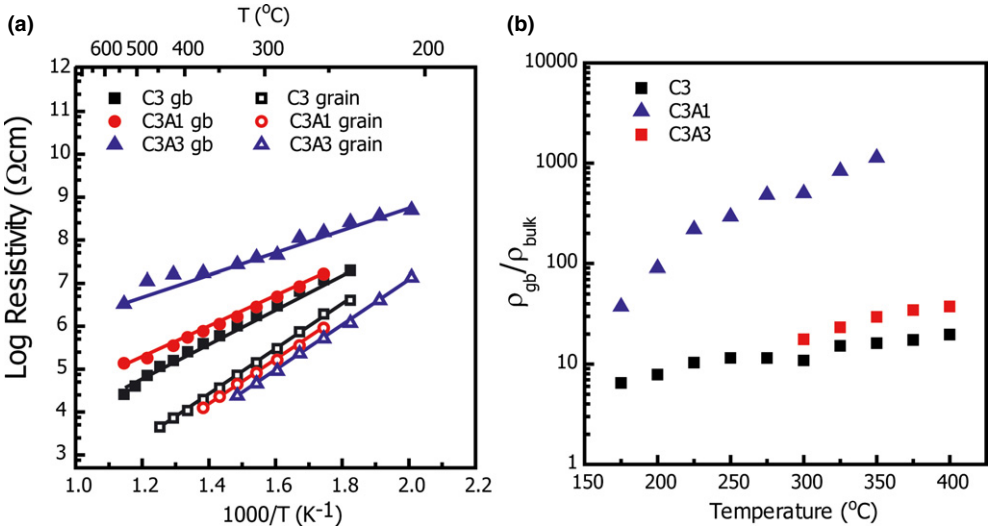

Fig. 4. (a) Electrical resistivity of the grain and grain boundary as a function of temperature for CaF_2-doped AlN ceramics with added Al_2O_3, and (b) the ratio of the grain-boundary resistivity to the grain resistivity. According to the addition of Al_2O_3, the grain-boundary resistivity and especially the ratio of the grain-boundary resistivity to the grain resistivity increase greatly.

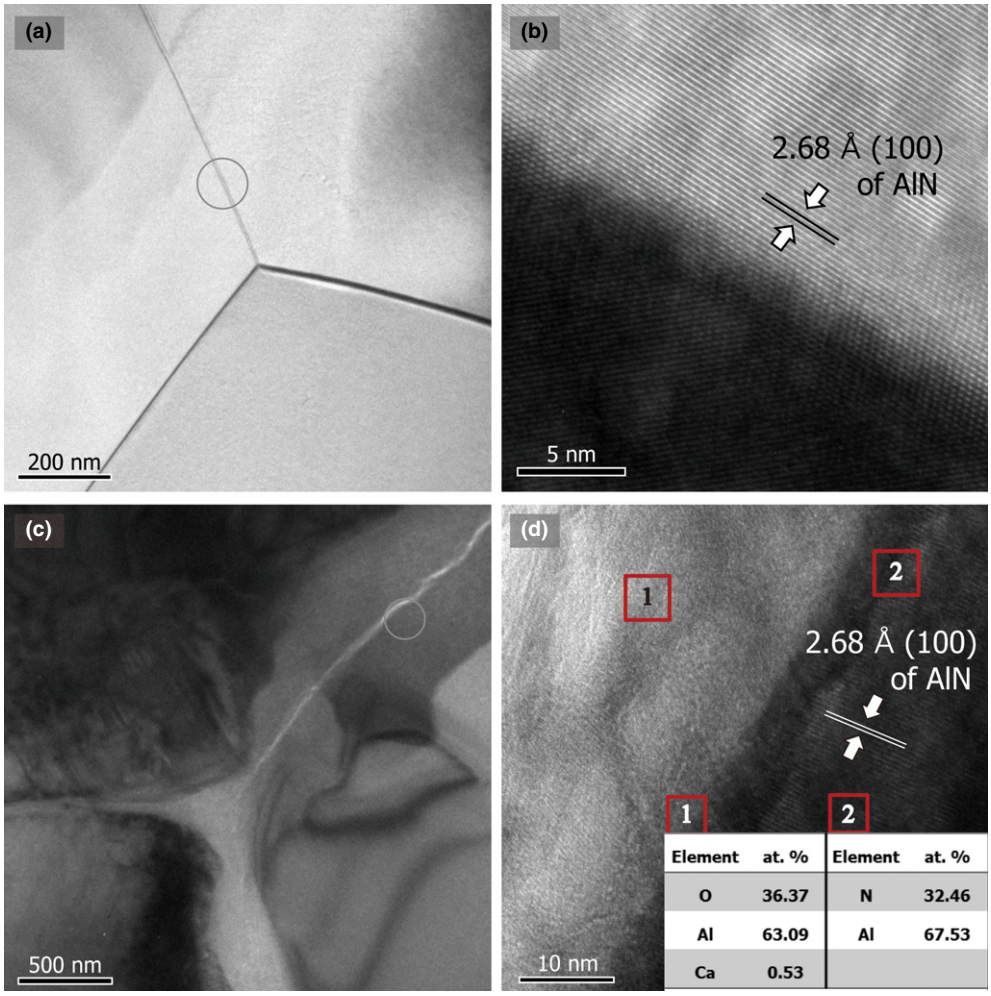

Fig. 5. TEM micrograph of specimens C3 (a)and C3A3 (c).HRTEM of C3 (b) and C3A3 (d) are the circled area of (a), (c). In the C3 specimen, the grain boundaries are essentially clean and there are no segregation atoms or amorphous/glassy phases along grain boundaries. In the C3A3 specimen, an amorphous phase occurred along grain boundaries, composed of Al, O, and small amounts of Ca.

space charge effect with charge carrier of AlN ceramics. It is well-known that the most dominant defects are oxygen-related defects in AlN ceramics, and aluminum vacancies or electron is generated according to oxygen incorporation into AlN lattice. From the very low ionic transference number (below 10^{-4}) in the results of Lee *et al.*, aluminum vacancies can be assumed to the main charge carrier.[20] So the grain-boundary resistivity is considered high because grain

boundaries block the ionic transport across them. This is usually called "the grain-boundary blocking effect". The blocking effect has often been mainly attributed to grain-boundary insulation phase, but the grain-to-grain contacts also can be blocking layer, suggesting an additional cause for the blocking effect ("intrinsic" effect). In the CaF_2–AlN system, the blocking nature can be accounted for the depletion of charge carriers, e.g., aluminum vacancies in the space charge layer of the AlN grain boundaries. According to the brick layer model, the grain-boundary resistivity can be interpreted in terms of a space charge layer adjacent the grain-boundary core in which the relevant charge carriers are depleted.

In the C3A3 specimen, anamorphous phase occurred along grain boundaries, composed of Al, O, and small amounts of Ca (0.53 at.%) [Fig. 5(c) and (d)]. HRTEM analysis of the C3A3 specimen showed that no other phase was observed between the amorphous phase and the AlN grain. The addition of additives including Al_2O_3 is known to cause an amorphous phase to form along grain boundaries.[18,21] To determine the effect of the amorphous phase at the grain boundary on the electrical resistivity, the activation energy of the grain and the grain resistivity were investigated. The grain activation energies of samples C3, C3A1, and C3A3 were 0.95, 1.06, and 1.09 eV, respectively. The concentration of charge carriers for electrical conduction in the C3A1 and C3A3 specimens changed compared with the concentration of the charge carriers in the C3 specimen, by transformation of Al_2O_3 solid solution into AlN grains during the sintering process. The grain-boundary activation energies of C3, C3A1, and C3A3 were 0.67, 0.44, and 0.37 eV, respectively. Low values of grain-boundary activation energy reveal that the CaF_2-doped AlN ceramics have a high electrical resistivity at high temperatures. Because Al_2O_3 adding specimens has not the grain-to-grain contact but the amorphous phase has the grain-boundary insulation phase, high grain-boundary resistivity and low activation energy can be explained as "extrinsic" grain-boundary blocking effect. The large difference in grain-boundary activation energy among the specimens indicates that the grain-boundary blocking mechanism for electrical conduction is different in each case. Microstructural analysis of C3A3 indicates that the specimen with added Al_2O_3 exhibits the grain-boundary blocking effect because of the presence of the amorphous phase.

The morphology of the amorphous phase can be represented by a discontinuous or continuous second-phase model in the electrical conduction mechanism.[20,22,23] In the continuous second-phase model, the interruption of contact by a thin layer of amorphous phase inclusions is assumed, with the covered grain-boundary area depending on the amount, composition, and wetting properties of the amorphous phase given the sintering conditions. The pathway through the intermediate amorphous phase is important in the case of extensive coverage by the amorphous phase. In this case, the grain-boundary activation energy should depend on the specific properties of the blocking phase. The activation energy should depend on the composition of the amorphous phase.[24] The difference in grain-boundary activation energy among the samples indicates that anamorphous phase exists at the grain boundary and acts as a blocking boundary. The large difference in grain-boundary activation energy between C3 and C3A3 is due to a continuous amorphous phase blocking boundary in the specimen doped with Al_2O_3. Considering the thermal conductivity results for C3 and C3A3, the thin amorphous phase at the grain boundary greatly increased the electrical resistivity of the AlN ceramics without a large deterioration in thermal conductivity. Therefore, the electrical resistivity of CaF_2-doped AlN can be controlled by the addition of a suitable amount of Al_2O_3, which enables the formation of a continuous amorphous phase along grain boundaries.

IV. Conclusion

Highly thermal conductive AlN ceramics without second phases were sintered with a CaF_2 sintering additive. The grain and grain-boundary resistivity of AlN were analyzed by applying the brick layer model. To control the electrical resistivity of the AlN grain boundary, an amorphous phase was produced at the boundary by adding Al_2O_3. The amorphous phase increased the electrical resistivity of the AlN ceramics, without decreasing the thermal conductivity. The grain-boundary resistivity of the specimens with added Al_2O_3 was two to four times higher than the grain resistivity. By adding Al_2O_3 to CaF_2-doped AlN ceramics, the electrical resistivity was controlled within the various experimental regimes. The different activation energies of grain-boundary resistivity in the various samples, combined with the results of microstructural analysis by TEM, revealed that the Al_2O_3- and CaF_2-doped AlN ceramics contained a continuous amorphous phase.

Acknowledgments

This study was supported by a grant from the Fundamental R&D Program for Core Technology of Materials funded by the Ministry of Commerce, Industry and Energy, Republic of Korea. This work was also partially supported by Basic Science Research Program through the National Research Foundation of Korea (NRF) funded by the Ministry of Education (2009-0094038).

References

[1]G. A. Slack, R. A. Tanzilli, R. O. Pohl, and J. W. Vandersande, "The Intrinsic Thermal Conductivity of AlN," *J. Phys. Chem. Solids*, **48**, 641–7 (1987).

[2]R. Bachelard and P. Joubert, "Aluminum Nitride by Carbothermal Reduction," *Mater. Sci. Eng., A*, **109**, 247–51 (1989).

[3]L. M. Sheppard, "Aluminum Nitride: A Versatile but Challenging Material," *Am. Ceram. Soc. Bull.*, **69** [11] 1801–10 (1990).

[4]L. Chouanine, M. Takano, F. Ashihara, and O. Kamiya, "Influence of the Surface Topography on the Micromechanical Properties and Performance of a CMP Finished AIN Component for Silicon Plasma Etching," *Adv. Fract. Fail. Prev.*, Pts 1 and 2, **261–263**, 1599–604 (2004).

[5]S. Kume, M. Yasuoka, N. Omura, and K. Watari, "Effects of Annealing on Dielectric Loss and Microstructure of Aluminum Nitride Ceramics," *J. Am. Ceram. Soc.*, **88** [11] 3229–31 (2005).

[6]M. Watanabe, Y. Mori, T. Ishikawa, T. Iida, K. Akiyama, K. Sawabe, and K. Shobatake, "X-ray Photoelectron Spectroscopy of Polycrystalline AIN Surface Exposed to the Reactive Environment of XeF_2," *Appl. Surf. Sci.*, **217** [1–4] 82–7 (2003).

[7]Y. Kurokawa, K. Utsumi, and H. Takamizawa, "Development and Microstructural Characterization of High-Thermal-Conductivity Aluminum Nitride Ceramics," *J. Am. Ceram. Soc.*, **71** [7] 588–94 (1988).

[8]K. Watari and K. Ishizaki, "Thermal Conduction Mechanism of Aluminum Nitride Ceramics," *J. Mater. Sci.*, **27**, 2627–30 (1992).

[9]W. J. Kim, D. K. Kim, and C. H. Kim, "Morphological Effect of Second Phase on the Thermal Conductivity of AlN Ceramics," *J. Am. Ceram. Soc.*, **79** [4] 1066–72 (1996).

[10]S. A. Jang and G. M. Choi, "Electrical-Conduction in Aluminum Nitride," *J. Am. Ceram. Soc.*, **76** [4] 957–60 (1993).

[11]H. S. Kim, J. M. Chae, Y. S. Oh, H. T. Kim, K. B. Shim, and S. M. Lee, "Effects of Carbothermal Reduction on the Thermal and Electrical Conductivities of Aluminum Nitride Ceramics," *Ceram. Int.*, **36** [7] 2039–45 (2010).

[12]R. W. Francis and W. L. Worrell, "High-Temperature Electrical-Conductivity of Aluminum Nitride," *J. Electrochem. Soc.*, **123** [3] 430–3 (1976).

[13]V. L. Richards, T. Y. Tien, and R. D. Pehlke, "High-Temperature Electrical-Conductivity of Aluminum Nitride," *J. Mater. Sci.*, **22** [9] 3385–90 (1987).

[14]J. Yoshikawa, Y. Katsuda, N. Yamada, C. Ihara, M. Masuda, and H. Sakai, "Effects of Samarium Oxide Addition on the Phase Composition, Microstructure, and Electrical Resistivity of Aluminum Nitride Ceramics," *J. Am. Ceram. Soc.*, **88** [12] 3501–6 (2005).

[15]T. Kusunose, T. Sekino, and K. Niihara, "Production of a Grain Boundary Phase as Conducting Pathway in Insulating AIN Ceramics," *Acta Mater.*, **55** [18] 6170–5 (2007).

[16]K. A. Khor, K. H. Cheng, L. G. Yu, and F. Boey, "Thermal Conductivity and Dielectric Constant of Spark Plasma Sintered Aluminum Nitride," *Mater. Sci. Eng. a-Struct.*, **347** [1–2] 300–5 (2003).

[17]H. K. Lee and D. K. Kim, "Defect Characterization of High Thermal Conductivity Caf_2 Doped Aln Ceramics by Raman Spectroscopy," *Mod. Phys. Lett. B*, **23** [31–32] 3869–76 (2009).

[18]E. Hagen, Y. D. Yu, T. Grande, R. Hoier, and M. A. Einarsrud, "Sintering of AlN Using CaO-Al_2O_3 as a Sintering Additive: Chemistry and Microstructural Development," *J. Am. Ceram. Soc.*, **85** [12] 2971–6 (2002).

[19]K. Watari, K. Ishizaki, and F. Tsuchiya, "Phonon-Scattering and Thermal Conduction Mechanisms of Sintered Aluminum Nitride Ceramics," *J. Mater. Sci.*, **28** [14] 3709–14 (1993).
[20]S. P. S. Badwal and A. E. Hughes, "The Effects of Sintering Atmosphere on Impurity Phase Formation and Grain Boundary Resistivity in Y_2O_3-Fully Stabilized ZrO_2," *J. Eur. Ceram. Soc.*, **10** [2] 115–22 (1992).
[21]H. Nakano, K. Watari, and K. Urabe, "Grain Boundary Phase in AlN Ceramics Fired Under Reducing N-2 Atmosphere with Carbon," *J. Eur. Ceram. Soc.*, **23** [10] 1761–8 (2003).
[22]S. P. S. Badwal and S. Rajendran, "Effect of Microstructures and Nanostructures on the Properties of Ionic Conductors," *Solid State Ionics*, **70**, 83–95 (1994).
[23]S. P. S. Badwal, "Grain-Boundary Resistivity in Zirconia-Based Materials - Effect of Sintering Temperatures and Impurities," *Solid State Ionics*, **76** [1–2] 67–80 (1995).
[24]X. Guo and J. Maier, "Grain Boundary Blocking Effect in Zirconia: A Schottky Barrier Analysis," *J. Electrochem. Soc.*, **148** [3] E121–6 (2001). □